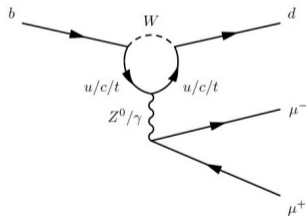


Direct Measurements of the Wilson Coefficients in the $B^\pm \rightarrow \pi^\pm \mu^+ \mu^-$ Decay with the LHCb detector

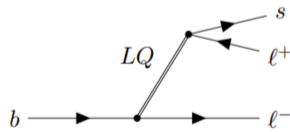
Xiaohan Wang¹, Michael McCann¹

¹Department of Physics
Imperial College London

- Various hints of the New Physics (NP) were observed in the rare $b \rightarrow sll$ transitions
 - E.g. angular observables distributions in $B^0 \rightarrow K^{*0} \mu^+ \mu^-$ [[PhysRevLett.125.011802](#)]
- It is also interesting to measure the similar $b \rightarrow dll$ transition
 - It is suppressed by the CKM matrix a ratio of $|V_{ts}/V_{td}|^2 \approx 22$ in the SM (Fig. 1a)
 - But can have a higher relative contribution from NP as in Fig. 1b
- The $B^\pm \rightarrow \pi^\pm \mu^+ \mu^-$ has only been measured for its BF in bins of dimuon mass squared (q^2) so far
- An unbinned q^2 method was developed for the $B^\pm \rightarrow K^\pm \mu^+ \mu^-$ [[CERN-THESIS](#)]
 - Maximise the sensitivity by fitting q^2 to extract the theoretical coefficient directly



(a) Loop Feynman diagrams of the $b \rightarrow d \mu^+ \mu^-$ decay predicted by the SM



(b) A possible NP Feynman diagram of $b \rightarrow d \mu^+ \mu^-$ decay with a leptoquark

An effective field theory (EFT) to be fitted in the q^2 spectrum to be model-independent

- Theoretical description of the $B^\pm \rightarrow \pi^\pm \mu^+ \mu^-$ decay over q^2 are functions of the Wilson parameters:

$$\frac{d\Gamma(B^\pm \rightarrow \pi^\pm \mu^+ \mu^-)}{dq^2} = F_{10}(C_{10}) + F_9(C_9^{eff}) + F_7(C_7^{eff}) \quad (1)$$

- For some functions $F_{7,9,10}$ of $C_{7,9,10}^{(eff)}$
- The vector and axial vector currents this analysis aims to measure C_9^{eff} and C_{10}
- C_9^{eff, B^\pm} encodes the **local rare decay** and **non-local components**

$$C_9^{eff, B^\pm}(q^2) = |C_9| e^{\pm i\phi_{C_9}} + \Delta C_9^{B^\pm}(q_0^2) + Y_{\rho, \omega}^{B^\pm}(q^2) + Y_{LQC}^{B^\pm}(q^2) + Y_{J/\psi, \psi(2S)}^{B^\pm}(q^2) \quad (2)$$

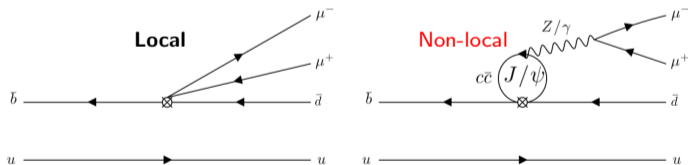


Figure: The Feynman diagrams of the **local rare decay** and a **non-local resonance**

Theoretical constraints

Due to the limited statistics available for the pion-final state, additional constraints are needed

- Detailed in [PhysRevD.109.116013]
- Simultaneously fit the data in $q^2 > 0$ and the theory predictions at $q < 0$
- Fit success rate increases significantly: 36% \rightarrow 78%

[PhysRevD.109.116013]

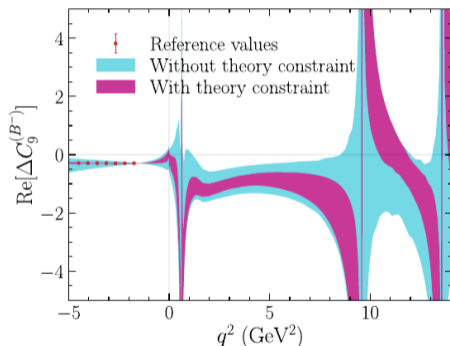


Figure: Non-local contribution for $B^- \rightarrow \pi^- \mu^+ \mu^-$ with and without the theoretical reference values as a constraint for x5 the expected LHCb Run1 + 2 pseudodatasets.

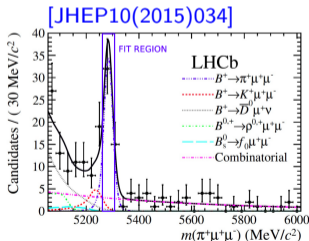
The differential decay rate, $\frac{d\Gamma_\mu}{dq_{true}^2}$ is constructed to a probability density function (PDF) $P(q_{rec}^2)$ as follows

- 1 Full Run1+Run2 data collected by the LHCb detector with an integrated luminosity of 8.3 fb^{-1}
- 2 $q^2 < 0$ theoretical constraint
- 3 $m_{\pi\mu\mu}$ is constrained to the known B-meson mass
- 4 A correction $\mathcal{E}(q^2)$ applied to account for selection
- 5 Convolved with a resolution function $\mathcal{R}(q_{rec}^2, q_{true}^2)$
- 6 Mis-identified (misID) and combinatorial backgrounds, $P_b(q_{rec}^2)$ added to the PDF
- 7 The PDF is fitted to the selected data to extract C_9 and ϕ_{C_9}

$$P(q_{rec}^2) = \mathcal{R}(q_{rec}^2, q_{true}^2) \otimes \left[\mathcal{E}(q_{true}^2) \frac{d\Gamma_\mu}{dq_{true}^2} \right] + \sum_{b=\text{misID}, \text{Comb.}} P_b(q_{rec}^2) \quad (3)$$

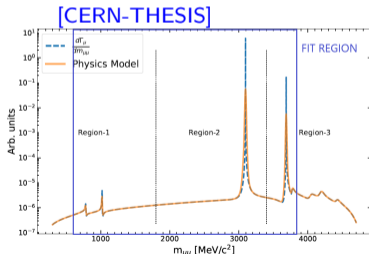
Selection and yields

- Most of the selections were derived from the binned analysis [JHEP10(2015)034]
 - Kaon has a factor of 25 larger decay rate, contributing a huge misID background \rightarrow a tight $m(\pi^\pm\mu^+\mu^-)$ mass cut
 - Pion final states are heavily contaminated by the combinatorial \rightarrow a dedicated combinatorial BDT was trained
 - Particle identity (PID) and combinatorial BDT cuts are re-optimised
 - The open-charm region is cut at $m_{\mu^+\mu^-} > 3750$ MeV/c² to avoid modelling more resonant parameters
- Signal, background modes this analysis includes:
 - Signal: $B^\pm \rightarrow \pi^\pm\mu^+\mu^-$, $J/\psi(\mu^+\mu^-)\pi^\pm$, $\psi(2S)(\mu^+\mu^-)\pi^\pm$
 - Background: $B^\pm \rightarrow K^\pm\mu^+\mu^-$, $J/\psi(\mu^+\mu^-)K^\pm$, $\psi(2S)(\mu^+\mu^-)K^\pm$ and Combinatorial
- Yields of each mode is estimated for pseudo-experiments (toys)
 - Yields of signal and misID modes are estimated from simulation
 - Yield of the combinatorial background is estimated with data in the upper-mass sideband (UMSB)



(a) The ± 40 MeV/c² fitted region in $m(\pi^\pm\mu^+\mu^-)$.

X.Wang (ICL)



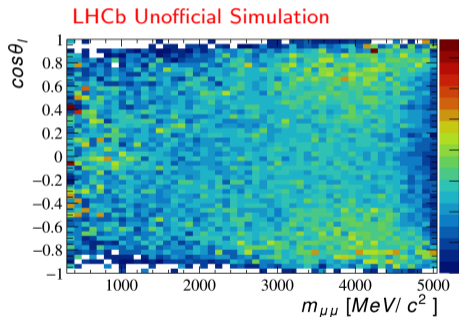
(b) The kaon equivalent dimuon mass spectrum adapted from

Modes	Yield
$\pi^\pm\mu^+\mu^-$	241
$J/\psi(\mu^+\mu^-)\pi^\pm$	55999
$\psi(2S)(\mu^+\mu^-)\pi^\pm$	35799
$K^\pm\mu^+\mu^-$	50
$J/\psi(\mu^+\mu^-)K^\pm$	8985
$\psi(2S)(\mu^+\mu^-)K^\pm$	2350
Combinatorial	1662

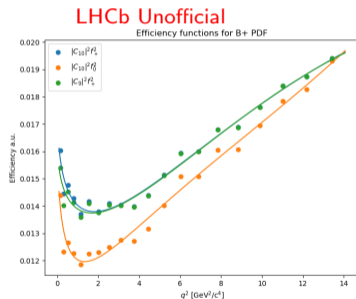
Table: Estimated yields of the signal, misID and combinatorial background modes

q^2 dependent efficiency function

- The PDF needs to be corrected for the experimental efficiency, which is dependent on q^2 and angles
- Efficiency at each q^2 bin is computed as the ratio of the generator-level and reconstructed-level simulation $\pi\mu\mu$ with the nominal selection
- The distribution is fitted with a 4th order polynomial (in $m_{\mu\mu}$)



(a) Efficiency distribution in $m_{\mu\mu}$ and $\cos\theta_l$

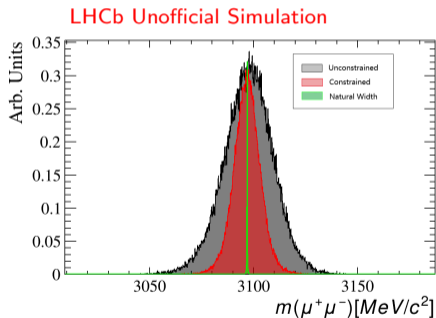


(b) Efficiency dependence in q^2 for B^+

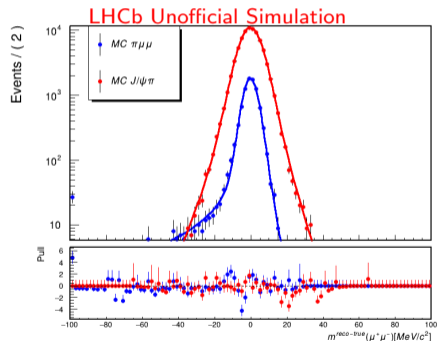
Resolution effect

The LHCb's $m_{\mu\mu}$ resolution is ~ 50 times wider than the natural J/ψ width, therefore:

- 1 A constraint on $m_{\pi\mu\mu}$ to the known B-mass
 - Effectively improve the resolution in $m_{\mu\mu}$ as shown in Fig. 6a
- 2 Resolution in $m_{\pi\mu\mu}$ is modelled and convolved with the theoretical differential decay rate
 - The resolution in the simulation is not perfect, so the resolution parameters are floated
 - From toys, the systematic effects of the shapes are $< 3\%$ of the statistical uncertainties of C_9 and ϕ_{C_9}



(a) Comparison of the J/ψ natural width, experimental widths before and after the $m_{\pi\mu\mu}$ constraint.



(b) Resolution functions for two regions in $m_{\pi\mu\mu}$.

- The only significant misidentified (misID) background modes are: $B^\pm \rightarrow J/\psi(\mu^+\mu^-)K^\pm$ and $B^\pm \rightarrow \psi(2S)(\mu^+\mu^-)K^\pm$
- A data-driven method is suggested to model the MisID shape
 - Using the kaon-like PID cuts to select pure kaon misidentified background in data
- Differences between this selection and the nominal selection are corrected
- Modelled with a double-sided Crystalball (DCB) added with a Gaussian function
- Shown with $B^\pm \rightarrow J/\psi(\mu^+\mu^-)K^\pm$ simulation in Fig. 7

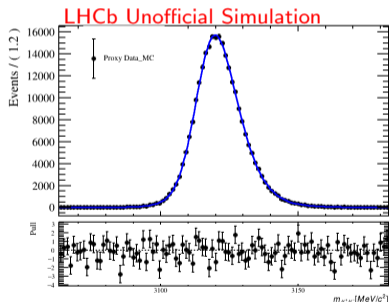
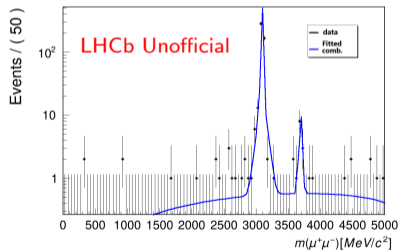


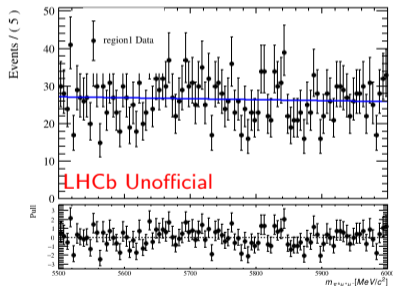
Figure: $J/\psi K$ simulation misID samples under the kaon PID selection, along with the fitted DCB + Gaussian function.

Shape of the combinatorial background

- Three components for the combinatorial background shape in $m_{\mu\mu}$ (Fig. 8a)
 - A double Gaussian with a common mean for the J/ψ resonant
 - A single Gaussian for the $\psi(2S)$ resonant
 - A ARGUS function for the non-resonant
- Fitting $m_{\mu\mu}$ using data in the UMSB
 - Equal width in $m_{\pi\mu\mu}$ to the data centered at $5460 \text{ MeV}/c^2$
 - Yields of each component are fixed, which are estimated from exponential extrapolation as in Fig. 8b
- Estimated systematic effects due to the combinatorial modelling are $< 5\%$ of the statistical uncertainties on C_9 and ϕ_{C_9}



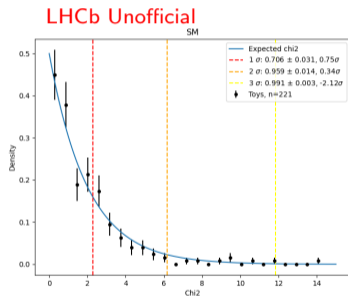
(a) Fitted combinatorial with double Gaussian J/ψ



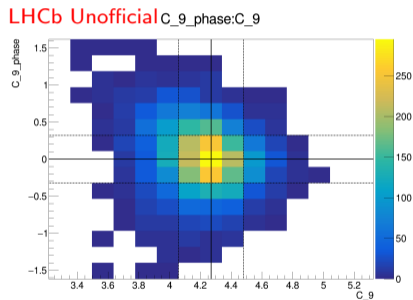
(b) Exponential fitted in the UMSB for the J/ψ region to estimate its yield.

To test whether the fit will produce good coverage or any bias, toys were generated for multiple tests

- Wilks' theorem: the likelihood difference follows the expected χ^2 distribution within 3σ
- Most likely point in the 2D histogram is at the generated value



(a) The density of the likelihood differences and the expected χ^2 curve from the Wilks' theorem. The $1 - 3\sigma$ regions of the χ^2 curve are shown in dashed lines in three colours.



(b) 2D histogram of fitted C_9 against ϕ_{C_9} from toys. The generated values are given in solid lines, and the statistical uncertainties are given in dashed lines.

- Extracting the Wilson parameters by fitting the q^2 spectrum of the rare $B^\pm \rightarrow \pi^\pm \mu^+ \mu^-$ decay
- A PDF is built based on the EFT, experimental resolution, and data-driven background modelling
- Toys and simulations are used to validate the PDF, coverage of the fit and systematic uncertainties
- The first direct measurement of physics parameters in the $b \rightarrow dll$ decay
- Approximate sensitivity: C_9/C_{10} : [+0.48 -0.46], ϕ_{C_9} : [+0.69 -0.71]

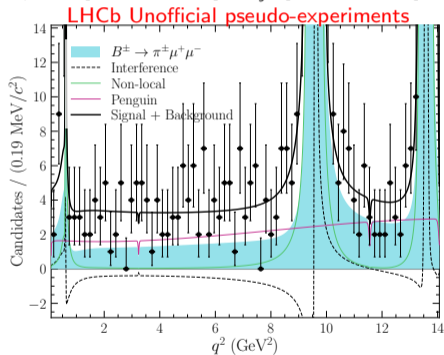


Figure: A toy with the expected yields generated from the overall B^\pm PDF with the Penguin (local), non-local and interference signal components highlighted.

1 Theory

2 Efficiency correction

3 Resolution

4 Combinatorial

5 Coverage

Differential decay rate and its components

Theoretical description of the $B^\pm \rightarrow \pi^\pm \mu^+ \mu^-$ decay over q^2 adapted is given as

$$\frac{d\Gamma(B^\pm \rightarrow \pi^\pm \mu^+ \mu^-)}{dq^2} = \frac{G_F^2 \alpha^2 |V_{tb} V_{td}^*|^2}{2^7 \pi^5} |\mathbf{k}| \beta_+ \left\{ \frac{2}{3} |\mathbf{k}|^2 \beta_+^2 |C_{10} f_+(q^2)|^2 + \frac{m_\ell^2 (M_B^2 - M_\pi^2)^2}{q^2 M_B^2} |C_{10} f_0(q^2)|^2 \right. \\ \left. + |\mathbf{k}|^2 \left[1 - \frac{1}{3} \beta_+^2 \right] \left| C_9^{eff, B^\pm} f_+(q^2) + 2 C_7^{eff} \frac{m_b + m_d}{M_B + M_\pi} f_T(q^2) \right|^2 \right\}$$

- $\beta(q^2) = \sqrt{1 - \frac{4m_l^2}{q^2}}$, $|\mathbf{k}| = \sqrt{E_\pi^2 - M_\pi^2}$
- $C_3^{eff} = C_7 - \frac{1}{3}(C_3 + \frac{4}{3}C_4 + 20C_5 + \frac{80}{3}C_6) + \mathcal{O}(\alpha_s)$
- Form factors from the HPQCD group [[PhysRevD.107.014510](#)]

$$f_{+,T}(q^2) = \frac{\mathcal{L}}{1 - q^2/M_{B_s^*}} \sum_{i=0}^{N-1} b_i^{+,T} [z^i - (-1)^{i-N} \left(\frac{i}{N}\right) z^N], \quad (4)$$

$$f_0(q^2) = \frac{\mathcal{L}}{1 - q^2/M_{B_s^*}} \sum_{i=0}^{N-1} b_i^0 z^i \quad (5)$$

- $z(q^2) = \frac{\sqrt{t_+ - q^2} - \sqrt{t_+ - t_0}}{\sqrt{t_+ - q^2} + \sqrt{t_+ - t_0}}$, $t_+ \equiv (M_B + M_\pi)^+$, $t_0 \equiv (M_B + M_\pi)(\sqrt{M_B} - \sqrt{M_K})^2$
- Coefficients $b_i^{0,+,T}$ are extracted from [[PhysRevD.93.025026](#)] with $N = 3$

Specifically, the effective C_9 goes as:

$$C_9^{eff, B^\pm}(q^2) = |C_9| e^{\pm i\phi_{C_9}} + \Delta C_9^{B^\pm}(q_0^2) + Y_{\rho, \omega}^{B^\pm}(q^2) \\ + Y^{B^\pm}(q^2)_{LQC}(q^2) + Y_{J/\psi, \psi(2S)}^{B^\pm}(q^2) + Y_{2P, c\bar{c}}(q^2)$$

- Vector resonances $Y_{\rho, \omega}^{B^\pm}(q^2)$, $Y_{J/\psi, \psi(2S)}^{B^\pm}(q^2)$
 - Each resonance is described by a relativistic Breit-Wigner distribution
- Two board shape q^2 distribution:

$Y_{LQC}(q^2)$: the light quark continuum

- rare mode ($V_{tb}V_{td}^*$), LQC ($V_{ub}V_{ud}^*$) both $\sim \lambda^3$ (LQC also includes c)
- LQC parameters are well known [1506.07760], but still floated for the fit

$Y_{2P, c\bar{c}}(q^2)$: the two-particle charmonium

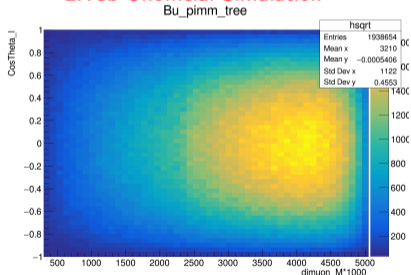
- re-scatterings $B^\pm \rightarrow \pi^\pm M_{j_1} M_{j_2} \rightarrow \pi^\pm \mu^+ \mu^-$
- $M_{j_1} M_{j_2} = \{DD, DD^*, D^* D^*\}$
- Each $M_{j_1} M_{j_2}$ contribution is described separately [2001.04470], but can be approximated with a single magnitude and phase parameter
- No D-meson due to the $m_{\mu\mu}$ cut, not included

- 1 Theory
- 2 Efficiency correction
- 3 Resolution
- 4 Combinatorial
- 5 Coverage

The efficiency from generator-level

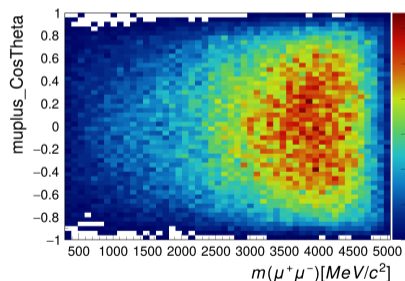
- The efficiency is both q^2 and angular dependent
 - Mainly due to the p_T on the muons and the IP on the hadron and dimuon
- More efficient at high $m_{\mu\mu}$ and $\cos\theta_l$ near 0
 - High efficiency at high $m_{\mu\mu}$: high efficiency on high p_T muons
 - Low efficiency at highest $m_{\mu\mu}$: strict IP requirement for a almost stationary kaon
 - Low efficiency at high $\cos\theta_l$ ($\theta_l \sim 0, \pi$): one fast and one slow muon
- Can we use the correction from the unbinned $K_{\mu\mu}$?
 - Some differences difficult to account for, e.g. different selection, phase space limits (4700 MeV vs 5050 MeV)

LHCb Unofficial Simulation



(a) Generator-level

LHCb Unofficial Simulation



(b) Reconstructed-level

- Despite the angular dependence being integrated out, it's relevant for the efficiency correction
- The full double differential decay rate:

$$\begin{aligned} \frac{d\Gamma_l}{dq^2 d\cos\theta_l} \propto & \sqrt{\lambda(q^2)} \beta \left\{ \frac{\lambda(q^2)}{4} \beta^2 (1 - \cos^2\theta_l^2) |C_{10}|^2 f_+^2(q^2) \right. \\ & + \frac{m_l^2}{q^2} (M_B^2 - M_K^2) |C_{10}|^2 f_0^2(q^2) \\ & \left. + \frac{\lambda(q^2)}{4} (1 - \beta^2 \cos^2\theta_l^2) |\tilde{C}_9|^2 f_+^2(q^2) \right\} \end{aligned}$$

- $\beta(q^2) = \sqrt{1 - 4m_l^2/q^2}$, where m_l is the muon rest mass
- The three terms have different angular dependence,
 - thus different efficiency correction once the angular is integrated out

- The efficiency correction \mathcal{E} corresponding to the three terms:

$$\mathcal{E}_{+C_{10}}(q^2) = \frac{\int_{-1}^{+1} \epsilon(q^2, \cos) (1 - \cos\theta_l^2) d\cos\theta_l}{\int_{-1}^{+1} (1 - \cos\theta_l^2) d\cos\theta_l} \quad (6)$$

$$\mathcal{E}_{0C_{10}}(q^2) = \frac{\int_{-1}^{+1} \epsilon(q^2, \cos) d\cos\theta_l}{\int_{-1}^{+1} d\cos\theta_l} \quad (7)$$

$$\mathcal{E}_{+C_{10}}(q^2) = \frac{\int_{-1}^{+1} \epsilon(q^2, \cos) (1 - \beta^2 \cos\theta_l^2) d\cos\theta_l}{\int_{-1}^{+1} (1 - \beta^2 \cos\theta_l^2) d\cos\theta_l} \quad (8)$$

- The efficiency weight $\epsilon(q^2, \cos\theta_l)$

$$\epsilon(m_{\mu\mu}, \cos\theta_l) = \sum_i \frac{\mathcal{N}_i^{J/\psi} N_i(m_{\mu\mu}, \cos\theta_l)}{\mathcal{N}_{2016}^{J/\psi} n_i(m_{\mu\mu}, \cos\theta_l)} \quad (9)$$

- N_i : reconstructed-level yield; n_i : generator-level yield; \mathcal{N}_i : $J/\psi K$ data yield
- $i \in [Run1, 2015, 2016, 2017, 2018]$, only relative year fractions matter
- For our analysis, can apply the year weights from the binned $\pi\mu\mu$ (normalised from $J/\psi K$)
- The three terms in decay rate are corrected separately before they are convolved with the resolution

$$P(q^2) = \mathcal{R}(q_{rec}^2, q_{true}^2) \circledast \left[\sum_i \mathcal{E}_i(q^2) \frac{d\Gamma_\mu^i}{dq^2} \right] \quad (10)$$

- 1 Theory
- 2 Efficiency correction
- 3 Resolution**
- 4 Combinatorial
- 5 Coverage

Fitted resolution parameters (for toys)

Individual fit

	$\pi\mu\mu$	$J/\psi\pi$	$\psi(2S)\pi$
α_L	1.50 ± 0.06	1.39 ± 0.03	1.34 ± 0.02
m_0	-0.08 ± 0.04	-0.22 ± 0.02	-0.37 ± 0.01
n_L	1.64 ± 0.11	17.94 ± 3.12	38.11 ± 7.71
n_R	13.61 ± 5.02	103.23 ± 72.45	20.01 ± 2.19
σ_{DCB}	3.64 ± 0.05	5.70 ± 0.03	5.17 ± 0.01

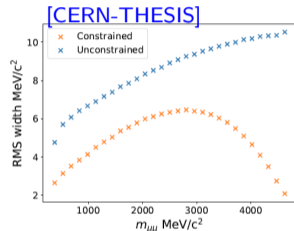
Simultaneous fit

	$\pi\mu\mu$ w. $J/\psi\pi$	$\psi(2S)\pi$ w. $J/\psi\pi$
α_L	1.44 ± 0.04	1.36 ± 0.01
m_0	-0.19 ± 0.02	-0.34 ± 0.01
n_L	15.35 ± 2.22	24.57 ± 4.46
n_L Flat	1.77 ± 0.07	32.34 ± 3.38
n_R	65.46 ± 35.20	140.30 ± 0.00000002
n_R Flat	16.38 ± 5.82	19.14 ± 0.89
σ_{DCB}	5.72 ± 0.02	5.68 ± 0.02
σ factor	0.63 ± 0.01	0.91 ± 0.0003

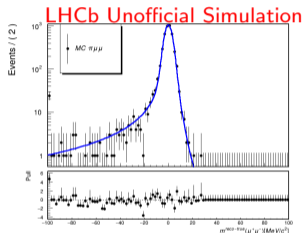
Difference in resolution within region-1

The resolution is different within the flat region-1, to quantify this...

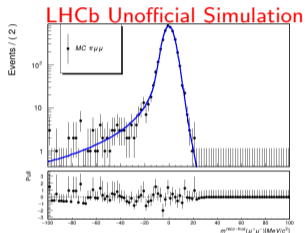
- Split at equal yields on both sides at $m_{\mu\mu} = 1295$ MeV



(a) Variation of the resolution in $m_{\mu\mu}$ for constrained and unconstrained B-mass.



(b) $\sigma_{DCB} = 3.11$ MeV



(c) $\sigma_{DCB} = 4.31$ MeV

- The width are different by +19%, -15% for the two regions compared with the full region
- A relatively big difference that is worth a systematic study

- Three systematics from the resolution interesting so far
 - ① Including a Gaussian to the resolution function or not
 - ② The “FFT gaps” between regions
 - ③ Difference in resolution in region-1
- For all three systematics, they are quantified with a similar approach to those from the combinatorial
 - ① Generated from DCB + Gaussian, fitted back with DCB only
 - ② Generated with one-region resolution, fitted back with three-region resolution, but share the same parameters
 - ③ Generated from upper-region-1 width, fitted back with lower-region-1 width (the region-1 width is not floated)
- All under the above toys setup, except not floating the form factors and the LQC, 150 toys each

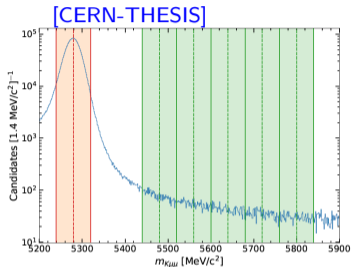
	C_9	C_9 pull	C_9 phase	C_9 phase pull
w/o Gaussian	0.005	-0.019	-0.01609	-0.0318
FFT gaps	0.006	0.0166	-0.002769	-0.00327
Upper/lower-region-1	0.001	0.0046	0.0097	0.03337

- All given as the difference between fitted with the original and alternative models
- A maximum of $\sim 3\%$ on the phase

- 1 Theory
- 2 Efficiency correction
- 3 Resolution
- 4 Combinatorial**
- 5 Coverage

Previous unbinned $K\mu\mu$ modelling of the combinatorial to account for the B mass constraint (*the UMSB extrapolation*)

- Split the UMSB in bins with widths equal to the signal window
- Model each bin with the same function, but fit the parameters
- Extrapolate the parameters linearly into the signal region



(a) $K\mu\mu$ analysis unconstrained and constrained B mass 2D

Adaptation of this method to the $\pi\mu\mu$ analysis

- The $\pi\mu\mu$ measurement is dominated by the statistical uncertainties,
 - So it might not be necessary to account for systematic like this
 - The systematic be tested with toys
- Low stats of combinatorial available for splitting the UMSB in bins and doing the extrapolation

To what extent do we care about the shape of the combinatorial?

- Use the toys to quantify the systematic
 - To quantify this, generate data D_0 with PDF F_0 , and fit back with both F_0 and F_1
 - Compare the difference between the fitted result from F_0 and F_1
 - The yield of the combinatorial of each component is chosen to be the same (because it's not determined from the fit)
- F_0 is chosen to be the same as in the $K\mu\mu$ analysis to represent the actual data
 - Assume a universal combinatorial shape
 - This is after the UMSB extrapolation, which is not capable for us (for now)
- Two alternative F_1 chosen: i.e. the single and double J/ψ Gaussian fits

F_1	C_9 Diff.	Pull Diff.	C_9 phase Diff.	Pull Diff.
Single Gaussian	+0.007	+0.0333	+0.01055	+0.0416
Double Gaussian	-0.012	-0.0552	+0.01204	+0.0454

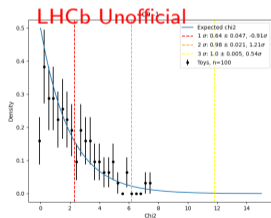
- Both can be considered to be small effect $O(1\%)$
- The single Gaussian is closer to the $K\mu\mu$ case as expected
- The signs of the two are flipped for C_9 , meaning:
 - the single-Gaussian *underestimate* the non-resonant combinatorial,
 - while the double-Gaussian *overestimate* the non-resonant combinatorial

- 1 Theory
- 2 Efficiency correction
- 3 Resolution
- 4 Combinatorial
- 5 Coverage**

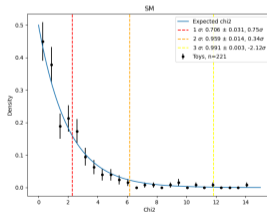
Wilks' theorem

Wilks theorem: under H_0 , the ratio of the likelihood follows a χ^2 distribution with d.o.f. equal to the difference in the number of parameters

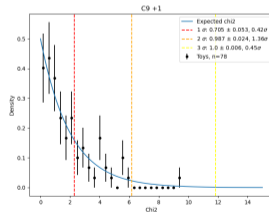
- i.e. do toy fit with/without the Wilson parameter floated
- It should follow a χ^2 with $k = 2$
- Necessary (but not sufficient) to show the likelihood surface has a good coverage
- In addition, it is tested with the actual number of toys within $1 - 3\sigma$ of χ^2
- Also need to show this is valid for different Wilson values, thus also tested for $C_9 = C_9^{SM} \pm 1$
- Can then assume the likelihood is not a strong function of the true values for points in between
- The largest deviation is -2.12σ within 3σ χ^2



(a) $C_9^{SM} - 1$



(b) SM



(c) $C_9^{SM} + 1$

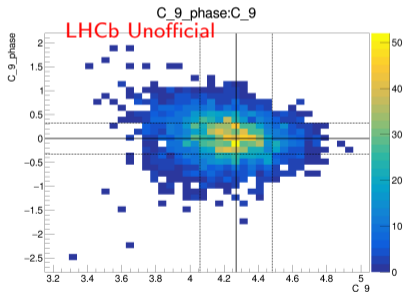
2D histogram

The Wilks test shows that the fitter has good coverage, but can we give the fitted value as a result?

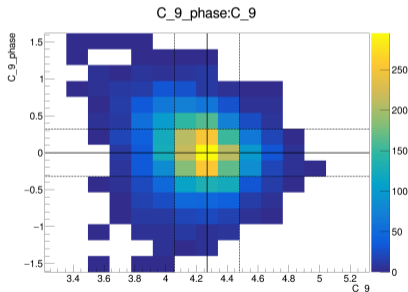
- The bias seen in the 1D might just be caused by the shape projection from the 2D
 - And we did see a “banana” shape that can negatively “bias” the C_9 in 1D
- We should look for the most likely bin in C_9 vs C_9 phase 2D histogram

But how certain are we about the bin being “the most likely”

- Start from large binning, reduce the binning in 2D simultaneously (a percentage of the error)
- Compare the difference in entries in the most likely bin N_1 , and the second-most bin N_2
- The significance: $(N_1 - N_2)/\sqrt{N_1}$



(a) Arbitrary binning



(b) The binning with a significance of 3.37,
 $C_9 : \pm 0.0726, \sim 0.69$ fitting error